# A Preliminary Exploration of Contribution of the Individual Rib to Dynamic Response of the Human Thorax

M. M. Murach[1], Y-S. Kang[1], J. Stammen[2], K. Moorhouse[2], J. H. Bolte IV[1], A. M. Agnew[1]

[1] Injury Biomechanics Research Center, The Ohio State University

[2] National Highway Traffic Safety Administration, Vehicle Research and Test Center

## ABSTRACT

*Rib fractures are still prevalent in motor vehicle crashes and a leading cause of morbidity and mortality. A large body of work has been undertaken to obtain thoracic and individual rib properties, but such testing has primarily focused on 50th percentile males and relies heavily on scaling to apply findings to other populations. Component level testing (i.e., individual bones) has the advantage of capturing large amounts of variation in subject level characteristics (sex, age, stature, etc.). To this end, 318 individual mid-level ribs from 168 post-mortem human subjects (4-108 years) were tested in a dynamic bending scenario simulating a frontal impact to the thorax. Although these data have allowed for an extensive exploration of variation in response of the rib, a gap remains in the ability to understand these findings in the context of the intact thorax. To address this, a series of non-injurious frontal impacts (20% chest compression) were conducted on three post-mortem human subjects. Each subject was tested in four sequential tissue states: intact with upper limbs, intact without upper limbs, denuded (superficial tissue removed), and eviscerated (superficial tissue and viscera removed). Force data were used to evaluate differences between the tissue conditions. Mid-level ribs were removed and tested to failure in the dynamic bending scenario previously described. Preliminary data presented here reveal that denuded thoraces retain approximately 80% of the intact peak force and stiffness, and the eviscerated thoraces retain approximately 45% of peak force and stiffness. Furthermore, the application of a model in which each rib is treated as a spring acting in parallel was developed in order to use individual rib response data to predict thoracic response. Initial analyses show the model has potential to predict eviscerated peak force and stiffness from cumulative rib response data. The ultimate goal is to develop a transfer function which utilizes the response of the individual rib to predict the response of the thorax from which it came, allowing for the generation of estimated thoracic response data for all populations. These data could be used to improve thoracic response targets and help assess the biofidelity of current anthropomorphic test devices.*

1

# INTRODUCTION

Although great strides have been made in improving frontal crash protection of the thorax, rib fractures are still prevalent and a leading cause of morbidity and mortality (Lee et al. 2015). To establish and improve response targets and injury thresholds, which are critical to the design and validation of biofidelic anthropomorphic test devices (ATDs) as well as finite element (FE) models, extensive thoracic testing must be conducted. Over the past several decades, a large body of work has obtained thoracic and individual rib properties. However, such testing has primarily focused on 50th percentile males (Nahum et al. 1971; Nahum et al. 1975; Ramet & Cesari 1979; Sacreste et al. 1982; Cesari & Bouquet 1990; Cavanaugh et al. 1993; Morgan et al. 1994; Yoganandan et al. 1995; Kent et al. 2003; Kent & Patrie 2005; Duma et al. 2006; Kemper et al. 2011) and relies heavily on scaling to apply findings to other populations (Mertz 1984; Maltese et al. 2010; Parent et al. 2010; Moorhouse 2013; Yoganandan et al. 2014).

FE models of the human body are increasingly being used to improve vehicle occupant protection and allow for manipulation of input data to create a model which represents populations not tested experimentally. In order to improve model validity, Kent 2008 conducted a study to determine guidelines which apportioned the contributions of thoracic components (superficial tissue, rib cage, and viscera) to the overall response. The author found that denuded thoraces retained approximately 60% of intact stiffness and eviscerated thoraces retained approximately 30% of their intact stiffness. However, this testing did not investigate the contribution of the individual rib to the intact thoracic response.

To better understand structural coupling and deformation patterns throughout the ribcage, Kindig et al. 2010 conducted experiments in which the ribs in a denuded and eviscerated thorax were loaded individually. The authors proposed a parallel spring model to represent the ribs in the thorax and found that ribs are more strongly coupled by side than by level. Since they did not conduct a full thoracic test and all tests were conducted at quasi-static rates, it is difficult to place rib response into the context of thoracic response, particularly in dynamic loading scenarios.

Component level testing (i.e., individual bones) has the advantage of capturing large amounts of human variation. For example, Schafman et al. tested 184 individual ribs from 93 post-mortem human subjects (PMHS) with ages ranging 4-99 years in a dynamic frontal loading scenario. The authors found that age and sex were only able to explain a small amount of variation in the structural response of the rib. Subsequent work has also found that most variation in rib response could not be explained by body size parameters (height, weight, and BMI) either. However, Murach et al. 2017 found that rib cross-sectional and gross geometry were able to successfully predict peak force and stiffness, indicating the importance of understanding the source of variation for individual rib properties.

To date, 318 individual mid-level ribs from 168 PMHS (4-108 years) have been tested, allowing for extensive exploration in variation between subjects, as well as between and within ribs. However, a gap remains in the ability to understand these findings in the context of the intact thorax. Therefore, the objective of this study was to begin preliminary investigations in order to develop a transfer function which utilizes the response of the individual rib to predict the response of the thorax from which it came using a hierarchical approach.

## METHODS

**Thoracic Hierarchy Testing**

A series of non-injurious frontal impacts were conducted on three male PMHS representing the 50th percentile male for height and weight (Table 1). Prior to impact, the subject was instrumented with strain gages at 30% and 60% of the rib curve length (measured from the vertebral end) at levels three through eight. The impacts were delivered using a pneumatic ram at a speed of 3m/s, corresponding to an approximate average strain rate of 0.5/s.

Table1: Subject Demographics

|  | Subject A | Subject B | Subject C |
|---|---|---|---|
| Sex | M | M | M |
| Age (years) | 73 | 62 | 55 |
| Stature (cm) | 170 | 173 | 183 |
| Mass (kg) | 62 | 84 | 75 |
| BMI (kg/cm$^2$) | 21.5 | 28.3 | 22.4 |
| aBMD t-score (lumbar) | 0.4 | 1.6 | 1.1 |
| Chest Depth (cm) | 20 | 24 | 20 |
| Chest Breadth (cm) | 33 | 34 | 31 |
| Chest Circumference (cm) | 90 | 108 | 95 |
| Thoracic Index | 0.61 | 0.71 | 0.65 |

*BMI = Body Mass Index (mass/stature$^2$), aBMD = areal bone mineral density as measured by dual-energy X-ray absorptiometry (DXA)

The ram impactor mass was 23 kg with a 6" high x 12" wide x 0.5" thick rectangular face centered vertically and horizontally on the sternum. The subject was tested in a fixed-back scenario for all impacts and chest deflection was calculated from a linear displacement potentiometer (Celesco CLWG-600-MC4, TE Connectivity Co., Berwyn, PA) attached to the impactor face. Chest depth was measured prior to each impact and the stroke of the ram was limited to <20% chest compression, as this is below the currently accepted threshold for thoracic injury (Kent 2008; Duma et al. 2006; Kemper et al. 2011).

Two 6-axis load cells (Denton 2944JFL, Humanetics, Plymouth, MI) were used to measure forces at the level of impact, with one attached to the impactor face (anterior) and one located behind the back plate (posterior). Both load cells were used in order to eventually compare these data to previous frontal thoracic work i.e., the force in an ATD frontal thorax impact test is typically measured anteriorly and the force in individual rib testing is measured posteriorly. To quantify the effect of all thoracic components, each subject was tested in four sequential tissue states: intact with upper limbs, intact without upper limbs, denuded (superficial tissue removed), and eviscerated (superficial tissue and viscera removed) (Figure 1).
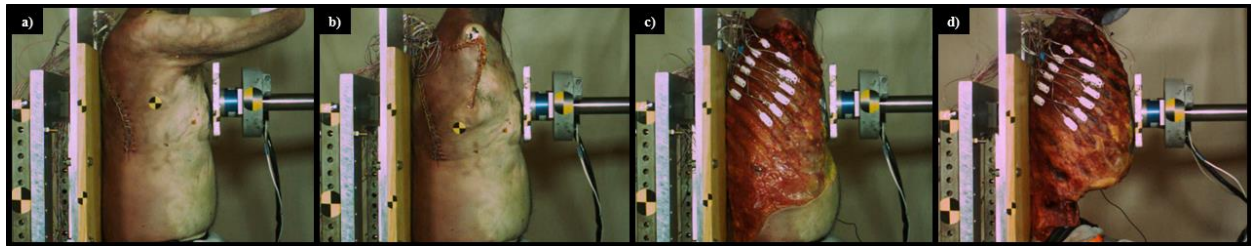
3

Figure 1: Experimental set-up for thoracic hierarchy testing in the four tissue states: a) intact with upper limbs b) intact without upper limbs c) denuded and d) eviscerated. Each image is at initial contact of the impactor face to the thorax.

**Individual Rib Testing**

Following eviscerated testing, bilateral pairs of ribs 4-7 were removed and tested to failure in a custom-built pendulum fixture (Figure 2) (Agnew et al. 2015; Schafman et al. 2016). The experiment simulated a frontal impact to the thorax in which the sternal (anterior) end of the rib was linearly translated toward the vertebral (posterior) end. A 54.4kg pendulum impacted ribs at 2m/s, resulting in an approximate strain rate of 0.5/s. Displacement of the sternal end of the rib was measured by a linear string potentiometer (Rayelco P-20A, AMETEK, Inc. Berwyn, PA), and forces were recorded by a 6-axis load cell (CRABI neck load cell, IF-954, Humanetics, Plymouth, MI) located posterior to the rib. The strain gages applied for thoracic testing remained in place for rib testing.
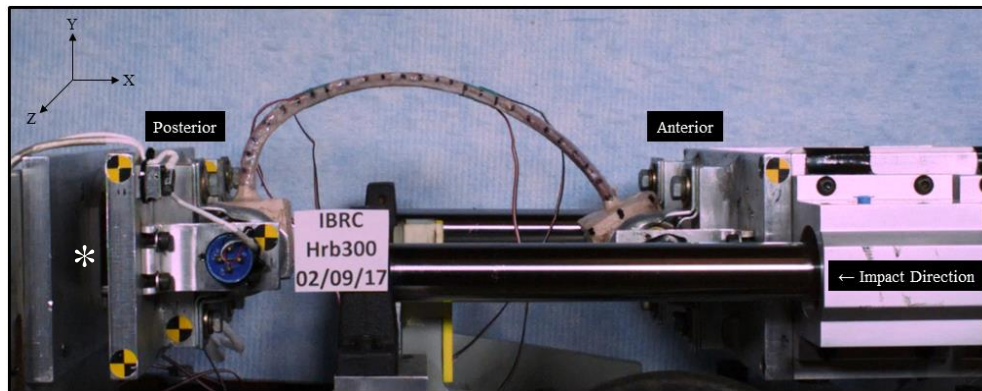


Figure 2: Experimental test setup for individual rib testing. Direction of impact is from right to left and the load cell is located behind the posterior plate, as indicated with an asterisk.

**Data Analysis**

All data were filtered using a CFC180 filter (SAE 2007). For the thoracic hierarchy, the anterior force data were inertially compensated using the mass and acceleration of the impactor face plate. A cumulative force response was calculated from the eight individual ribs tested from each thorax by multiplying the force in the primary loading direction (X) generated during each rib test by the cosine of rib angle and then summing the data according to Equation 1. A cumulative deflection response was calculated by averaging the displacement across the rib tests according to Equation (2). Because of the nature of the model, all individual rib data had to be

4

truncated according to the rib with the shortest time to failure. Rib angle was measured by estimating a line along the rib length on a 2D lateral image of the seated subject in the eviscerated condition, and then measuring the angle of that line with respect to horizontal. This method of analysis treats each rib as a spring acting in parallel with the remaining ribs in the thorax, similar to the analysis presented by Kindig et al. 2010.

$$Force = \sum_{i=1}^{n} F_n(t) \tag{1}$$

$$Displacement = \frac{1}{n}\sum_{i=1}^{n} D_n(t) \tag{2}$$

Since all subjects were limited to 20% chest deflection, a simplified stiffness value reflecting the differences in response data was calculated by dividing peak force by peak deflection. Differences in peak forces and stiffness values within subjects were quantified by dividing the measured peak force of each tissue condition by the baseline condition (intact with upper limbs), referred to as the force fraction here. The resulting values are interpreted as the amount of force or stiffness that each tissue condition retained when compared to the baseline. The ability of the cumulative rib model to represent the thorax was calculated by dividing the cumulative rib model peak force (or stiffness) by the eviscerated peak force (or stiffness).


## RESULTS

**Thoracic Hierarchy Testing**

Time histories for forces recorded by the anterior and posterior load cells for all tissue states of Subjects A-C can be found in Figure 3, and peak force values are shown in Table 2. Qualitatively, removal of the upper limbs had a minimal effect on the resulting anterior force data, and subsequent tissue removal resulted in a decrease in the overall response.
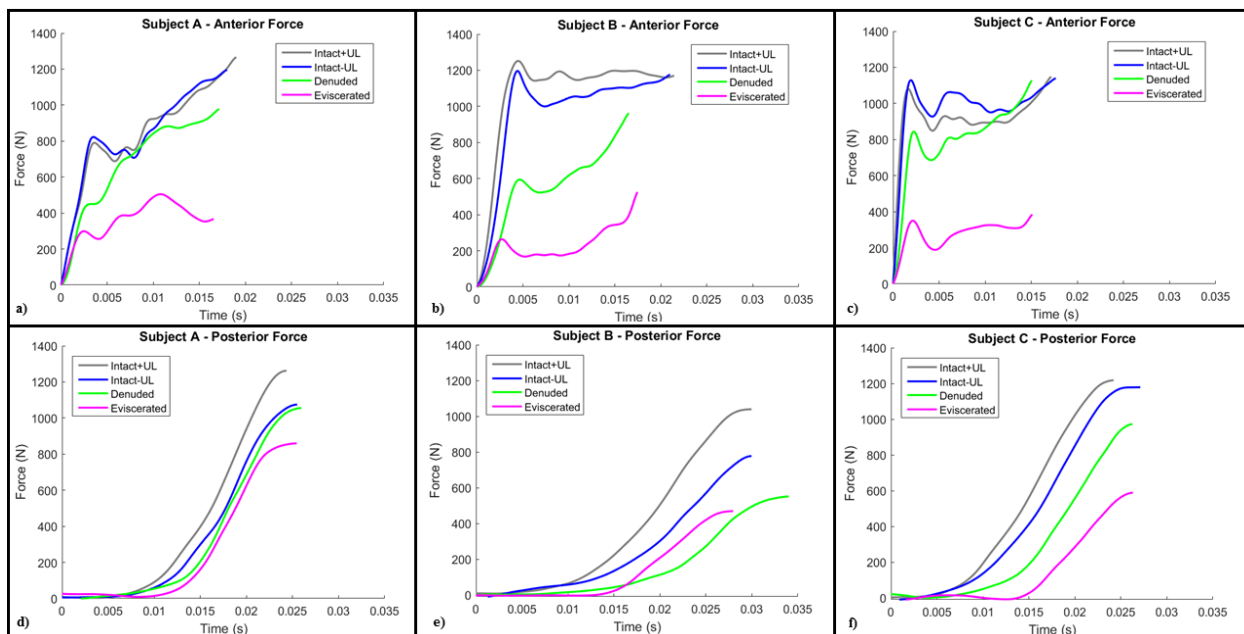
5

Figure 3: Force time histories from thoracic hierarchy testing of Subject A (left), B (center), and C (right) recorded by the anterior (top row) and posterior (bottom row) load cell. Response for each condition is included: gray = intact including upper limbs, blue = intact excluding upper limbs, green = denuded, and pink = eviscerated. All force data were cut at peak.

Table 2: Peak force values from thoracic hierarchy testing

| Anterior Load Cell Peak Force (N) | | | | | | | |
|---|---|---|---|---|---|---|---|
| | Intact + UL | Intact - UL | | Denuded | | Eviscerated | |
| Subject | Force (baseline) | Force | *Force Fraction* | Force | *Force Fraction* | Force | *Force Fraction* |
| A | 1247.4 | 1195.8 | *0.96* | 937.3 | *0.75* | 504.9 | *0.40* |
| B | 1170.0 | 1146.3 | *0.98* | 889.1 | *0.76* | 370.7 | *0.32* |
| C | 1096.3 | 1125.4 | *1.03* | 1069.4 | *0.98* | 325.7 | *0.30* |
| Average | 1171.2 | 1155.9 | *0.99* | 965.3 | *0.83* | 400.4 | *0.34* |
| St. Dev. | 61.7 | 29.5 | *0.03* | 76.2 | *0.10* | 76.1 | *0.05* |
| Posterior Load Cell Peak Force (N) | | | | | | | |
| | Intact + UL | Intact - UL | | Denuded | | Eviscerated | |
| Subject | Force (baseline) | Force | *Force Fraction* | Force | *Force Fraction* | Force | *Force Fraction* |
| A | 1270.9 | 1083.4 | *0.85* | 1068.4 | *0.84* | 864.8 | *0.68* |
| B | 1041.4 | 789.6 | *0.76* | 560.1 | *0.54* | 479.6 | *0.46* |
| C | 1231.3 | 1181.4 | *0.96* | 992.0 | *0.81* | 599.2 | *0.49* |
| Average | 1181.2 | 1018.1 | *0.86* | 873.5 | *0.73* | 647.8 | *0.54* |
| St. Dev. | 100.2 | 166.5 | *0.08* | 223.8 | *0.14* | 161.0 | *0.10* |

6

It should be noted that Subject B was found to have incomplete (i.e. not through both cortices) rib fractures located near the costochondral junction at autopsy. Strain gage data revealed that these fractures occurred during the intact without upper limbs impact (baseline). Since these fractures occurred in the first impact, subsequent responses and relative differences with respect to that initial impact configuration were still compared within Subject B. Subject A and C did not experience any rib fractures.

Peak forces decrease within each subject as tissue is removed. The differences in peak force due to the removal of the upper limbs indicates the effect of this procedure is negligible when using data from the anterior load cell, but not the posterior. On average using either anterior and posterior load cell, the denuding procedure resulted in the thorax retaining 78% of its intact force response and the eviscerating procedure resulted in the thorax retaining only 44% of its intact force response.

**Individual Rib Testing**

Time histories for force from each individual rib test can be found in Figure 4, and peak force values are shown in Table 3. In general, it appears that the lower level ribs tend to be stiffer than upper level ribs.
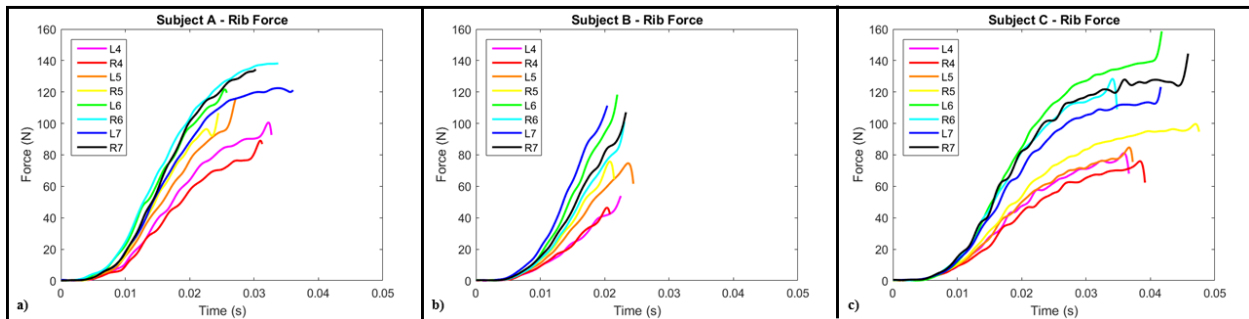


Figure 4: Force time histories from individual rib testing. Data are cut at time of fracture, determined by strain gage output.

Table 3: Peak force values from individual rib testing and the cumulative rib model

| Ride Side & Level | Peak Force (N) | | |
|---|---|---|---|
| | Subject A | Subject B | Subject C |
| L4 | 100.6 | 53.9 | 81.1 |
| R4 | 89.0 | 46.4 | 76.0 |
| L5 | 116.0 | 74.7 | 84.7 |
| R5 | 106.6 | 75.8 | 99.7 |
| L6 | 121.6 | 118.3 | 158.6 |
| R6 | 138.2 | 101.0 | 128.4 |
| L7 | 122.5 | 111.3 | 123.2 |
| R7 | 134.4 | 107.1 | 144.4 |
| **Cumulative Model** | **671.7** | **482.6** | **551.7** |

7

**Cumulative Rib Model**

The average angles of ribs 4-7 for Subject A, B, and C were 33.6°, 33.3°, and 46.3°, respectively. Due to the nature of the model, all individual rib data had to be truncated according to the rib with the shortest time to failure, resulting in peak forces of the cumulative rib model ranging from 482-672N (Table 3). Time histories for force from the cumulative rib model compared to those for all thoracic tissues states are shown in Figure 5.
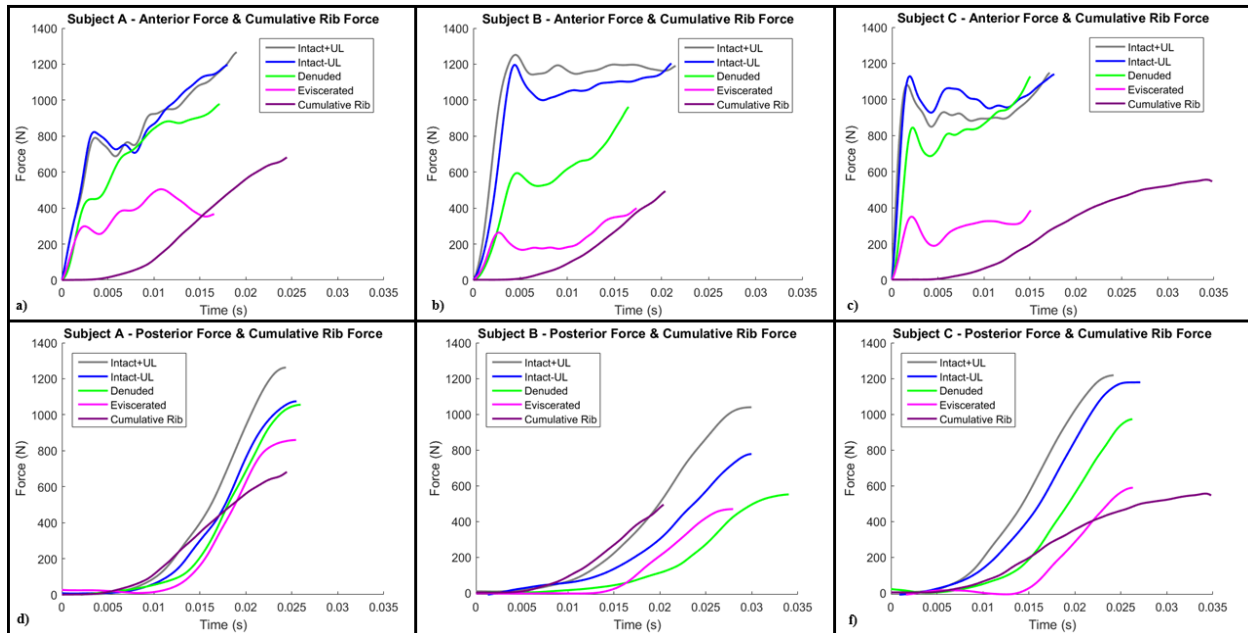


Figure 5: Force time histories from thoracic hierarchy testing of Subject A (left), B (center), and C (right) recorded by the anterior (top row) and posterior (bottom row) load cell with the cumulative rib model included. Response for each condition is included: gray = intact including upper limbs, blue = intact excluding upper limbs, green = denuded, pink = eviscerated, and purple = rib.

The cumulative rib model resulted in greater peak forces than those measured by the anterior load cell (average force fraction = 1.44) for the eviscerated thoracic condition. However, the cumulative rib model performed better (average force fraction = 0.90) when compared to the posterior load cell thoracic data (Table 4).

Table 4: Comparison of peak forces from eviscerated thoracic testing and cumulative rib models

| Anterior Load Cell Peak Force (N) | | | |
|---|---|---|---|
| Subject | Eviscerated | Cumulative Rib | *Force Fraction* |
| A | 504.8 | 671.7 | *1.33* |
| B | 370.7 | 482.6 | *1.30* |
| C | 325.8 | 551.7 | *1.69* |
| Average | 400.4 | 568.7 | *1.44* |
| St. Dev. | 76.0 | 78.1 | *0.18* |
| Posterior Load Cell Peak Force (N) | | | |
| Subject | Eviscerated | Cumulative Rib | *Force Fraction* |
| A | 864.8 | 671.7 | *0.78* |
| B | 479.6 | 482.6 | *1.01* |
| C | 599.1 | 551.7 | *0.92* |
| Average | 647.8 | 568.7 | *0.90* |
| St. Dev. | 161.0 | 78.1 | *0.09* |

Since all subjects were limited to 20% chest deflection, a simplified stiffness value reflecting the differences in response data was calculated by dividing peak force by peak deflection (Table 5). On average from both load cells, denuding resulted in the thorax retaining 80% of its intact stiffness and eviscerating resulted in stiffness retention of 44%. Stiffness values of the cumulative rib models were typically considerably higher than those obtained from eviscerated thoracic testing (Table 6).

9

Table 5: Stiffness values from thoracic hierarchy testing

| Anterior Load Cell Stiffness (N/mm) | | | | | | | | |
|---|---|---|---|---|---|---|---|---|
| Subject | Intact + UL Stiffness (baseline) | Intact - UL | | Denuded | | Eviscerated | | |
| | | Stiffness | *Stiffness Fraction* | Stiffness | *Stiffness Fraction* | Stiffness | *Stiffness Fraction* | |
| A | 25.92 | 24.65 | *0.95* | 19.38 | *0.75* | 6.97 | *0.27* | |
| B | 21.19 | 20.81 | *0.98* | 18.86 | *0.89* | 6.76 | *0.32* | |
| C | 28.77 | 27.10 | *0.94* | 23.69 | *0.82* | 7.22 | *0.25* | |
| Average | 25.3 | 24.2 | *0.96* | 20.6 | *0.82* | 7.0 | *0.28* | |
| St. Dev. | 3.1 | 2.6 | *0.02* | 2.2 | *0.06* | 0.2 | *0.03* | |

| Posterior Load Cell Peak Stiffness (N/mm) | | | | | | | | |
|---|---|---|---|---|---|---|---|---|
| Subject | Intact + UL Stiffness (baseline) | Intact - UL | | Denuded | | Eviscerated | | |
| | | Stiffness | *Stiffness Fraction* | Stiffness | *Stiffness Fraction* | Stiffness | *Stiffness Fraction* | |
| A | 24.63 | 21.51 | *0.87* | 21.45 | *0.87* | 17.33 | *0.70* | |
| B | 19.24 | 14.32 | *0.74* | 11.16 | *0.58* | 8.80 | *0.46* | |
| C | 26.04 | 24.59 | *0.94* | 21.51 | *0.83* | 12.27 | *0.47* | |
| Average | 23.3 | 20.1 | *0.85* | 18.0 | *0.76* | 12.8 | *0.54* | |
| St. Dev. | 2.9 | 4.3 | *0.08* | 4.9 | *0.13* | 3.5 | *0.11* | |

Table 6: Comparison of stiffness from eviscerated thoracic testing and cumulative rib models

| Anterior Load Cell Stiffness (N/mm) | | | |
|---|---|---|---|
| Subject | Eviscerated | Cumulative Rib | *Stiffness Fraction* |
| A | 6.97 | 23.14 | *3.32* |
| B | 6.76 | 23.20 | *3.43* |
| C | 7.22 | 11.98 | *1.66* |
| Average | 7.0 | 19.4 | *2.80* |
| St. Dev. | 0.2 | 5.3 | *0.81* |

| Posterior Load Cell Stiffness (N/mm) | | | |
|---|---|---|---|
| Subject | Eviscerated | Cumulative Rib | *Stiffness Fraction* |
| A | 17.33 | 23.14 | *1.34* |
| B | 8.80 | 23.20 | *2.64* |
| C | 12.27 | 11.98 | *0.98* |
| Average | 12.8 | 19.4 | *1.65* |
| St. Dev. | 3.5 | 5.3 | *0.71* |

## DISCUSSION

Across all subjects, tissue removal resulted in a decrease in thoracic force and stiffness. On average from using either load cell, the denuded thoraces retained approximately 80% of the intact peak force and the eviscerated thoraces retained approximately 45%. Similarly, the denuded thoraces retained nearly 80% of the intact stiffness and the eviscerated thoraces retained approximately 45% as well. This is expected because this stiffness value was calculated by dividing peak force by peak deflection, which was controlled to be the same within each subject.

Focusing on the posterior load cell, the reductions in stiffness are less than those found by Kent 2008, who found that denuded thoraces retained approximately 60% of their intact stiffness (and eviscerated thoraces retained approximately 30% of their intact stiffness by measuring force posteriorly. This could potentially be due to rate differences (Kent 2008 tested at ~1m/s), subject differences (Kent 2008 tested two female subjects), and testing configuration (Kent 2008 tested the subjects laying supine with a material testing system). Additionally, it should be noted that although the removal of the upper limbs did not appear to influence the anterior force data (average anterior force fraction = 0.99), it did have an effect on the posterior force data (average posterior force fraction = 0.86), potentially due to the mass of the arms and the interaction of the scapulae with the back plate. Kent 2008 left the upper limbs on for all tissue states, which may have also contributed to the differences found between the studies.

The cumulative rib model worked best when compared to posterior load cell forces in thoracic hierarchy testing, since the model consistently showed higher peak forces than the eviscerated values from the anterior load cell. This finding is not surprising, as forces are recorded by a posterior load cell during individual rib testing (Figure 1). The cumulative rib model had consistently higher stiffness values than the eviscerated test stiffness values calculated from both the anterior and posterior load cell during thoracic hierarchy testing. This is likely due to the differences in deflection in the thoracic hierarchy testing compared to individual rib testing (i.e., limited to 20% vs. tested to failure). Furthermore, the cumulative rib model presented here assumed that ribs are fully coupled, meaning that if a displacement was applied to one rib while in the thorax, the remaining ribs would displace the same amount. However, Kindig et al. 2010 found that although the ribs were fully coupled bilaterally, the degree of coupling decreased with rib level (upper ribs were more strongly coupled than lower ribs), which is likely due to the varying connections of the ribs to the sternum via costal cartilage. Future work will explore different methods for calculating stiffness as well as other ways to relate individual rib data to eviscerated thorax response.

Although the testing was designed to be non-injurious, Subject B experienced rib fractures in L4, L5, R5, and R6 in the intact with upper limbs impact (baseline), confirmed with strain gage data. The fractures occurred anteriorly at the costochondral junction allowing for the individual ribs to still be tested, because the fractures were embedded within the rib-end potting material. Since these fractures occurred in the first impact, subsequent responses and relative differences with respect to that initial impact configuration may still be comparable within subject B, especially since fractures were incomplete (i.e., not through both cortices) meaning a connection of the bone remained; however, peak force magnitudes and stiffness values should be utilized with caution because progression of the fracture in each successive test is assumed to be stable throughout the test series. For example, peak forces for subject B are all lower than subject A and C (Table 3) and rib responses appear to lack a plastic response (Figure 4). However, it is difficult to say if these differences are due to rib fracture or simply individual

11

variation. Surprisingly, Subject B had the highest aBMD t-score, which is the current metric for bone quality, indicating that this subject should not have experienced fractures.

Although these data offer potential for understanding contributions of individual ribs to thoracic response, there are several limitations. Thoracic testing was limited to 20% chest compression to allow for repeated non-injurious impacts, meaning the response data does not represent a full impact where the ram would be allowed to displace until all input energy is absorbed. Despite this, fractures still occurred for one subject. Additionally, all tests were completed using a fixed back scenario, which is not a realistic representation of a car crash scenario in which the forward inertia of occupants plays an important role. Although the angle of the rib was factored into the cumulative rib model, the model does not account for off-axis loading or rotation of the ribs with respect to the spine during thoracic hierarchy testing, both of which are likely important for establishing an accurate model. Future work will include additional testing to further improve understanding of the effects of denuding and eviscerating. Additionally, more complex methods of calculating thoracic stiffness will be investigated, as well as more intricate thoracic models that incorporate damping and inertial terms. Alternative cumulative rib models will be explored that incorporate individual rib force, displacement, angle, and strain.

## CONCLUSIONS

Preliminary data presented here reveal that denuded thoraces retain approximately 80% of the intact peak force and stiffness, and the eviscerated thoraces retain approximately 45% of peak force and stiffness. The cumulative rib model shows promise when utilized in context of the posterior load cell force in thoracic testing. These data will be useful for developing a transfer function to allow for the prediction of thoracic response from individual rib data, to allow for the generation of thoracic response data for populations for which full-thoracic impacts are not typically conducted (e.g., pediatric) but individual rib testing can be. These data could be used to improve thoracic response targets and help assess the biofidelity of ATDs of all sizes and demographics.

## ACKNOWLEDGEMENTS

## REFERENCES

Agnew, A.M. et al., 2015. The Effect of Age on the Structural Properties of Human Ribs. *Journal of the Mechanical Behavior of Biomedical Materials*, 41, pp.302–314.

Cavanaugh, J.M. et al., 1993. Injury and Response of the Thorax in Side Impact Cadaveric Tests. *Stapp Car Crash Conference*, 37, pp.199–221.

Cesari, D. & Bouquet, R., 1990. Behavior of Human Surrogates Thorax under Belt Loading. *SAE*

*International*, 902310, pp.73–81.

Duma, S.M. et al., 2006. Non-Censored Rib Fracture Data From Dynamic Belt Loading Tests on the Human Cadaver Thorax. *Biomedical Sciences Instrumentation*, 42, pp.148–153.

Kemper, A.R. et al., 2011. Reducing Chest Injuries in Automobile Collisions: Rib Fracture Timing and Implications for Thoracic Injury Criteria. *Annals of Biomedical Engineering*, 39(8), pp.2141–2151.

Kent, R., 2008. Frontal Thoracic Response to Dynamic Loading: The Role of Superficial Tissues, Viscera and the Rib Cage. *International Journal of Crashworthiness*, 13(3), pp.289–300.

Kent, R. & Patrie, J., 2005. Chest Deflection Tolerance to Blunt Anterior Loading is Sensitive to Age but Not Load Distribution. *Forensic Science International*, 149(2–3), pp.121–128.

Kent, R.W., Patrie, J. & Benson, N., 2003. Restrained Hybrid III Dummy-Based Criteria for Thoracic Hard Tissue Injury Prediction. In *International Conference on the Biomechanics of Impact*. pp. 215–232.

Kindig, M.W. et al., 2010. Structural Response of Cadaveric Ribcages under a Localized Loading: Stiffness and Kinemamtic Trends. *Stapp Car Crash Conference*, 54, pp.337–380.

Lee, E.L., Craig, M. & Scarboro, M., 2015. Real-World Rib Fracture Patterns in Frontal Crashes in Different Restraint Conditions. *Traffic Injury Prevention*, 16(sup2), pp.S115–S123. Available at: http://www.tandfonline.com/doi/full/10.1080/15389588.2015.1062888.

Maltese, M.R. et al., 2010. Incorporation of CPR Data into ATD Chest Impact Response Requirements. *Annals of Advances in Automotive Medicine*, 54(Figure 1), pp.79–88.

Mertz, H.J., 1984. A Procedure for Normalizing Impact Response Data. *Society of Automotive Engineers*.

Moorhouse, K., 2013. An Improved Normalization Methodology for Developing Mean Human Response Curves. Proc. of *23rd International Technical Conference on the Enhancced Safety of Vehicles*. Paper No. 13-0192.

Morgan, R.M. et al., 1994. Thoracic Trauma Assessment Formulations for Restrained Drivers in Simulated Frontal Impacts. *Stapp Car Crash Journal*, 38, pp.15–34.

Murach, M.M. et al., 2017. Rib Geometry Explains Variation in Dynamic Structural Response: Potential Implications for Frontal Impact Fracture Risk. *Annals of Biomedical Engineering*.

Nahum, A. et al., 1971. The Biomechanical Basis for Chest Impact Protection: I. Force-Deflection Characteristics of the Thorax. *Journal of Trauma*, 11(10), pp.874–882.

Nahum, A., Schneider, D. & Kroell, C., 1975. Cadaver Skeletal Response to Blunt Thoracic Impact. *Stapp Car Crash Conference*, 19, pp.259–293.

Parent, D.P. et al., 2010. Comparison of Hybrid III Child Test Dummies to Pediatric PMHS in Blunt Thoracic Impact Response. *Traffic Injury Prevention*, 11(4), pp.399–410.

Ramet, M. & Cesari, D., 1979. Behavior of Restrained Dummies and Cadavers in Frontal Impacts. In *International Conference on the Biomechanics of Impact*. pp. 210–222.

Sacreste, J. et al., 1982. Proposal for a Thorax Tolerance Level in Side Impacts Based on 62 Tests Performed with Cadavers Having Known Bone Condition. In *Stapp Car Crash Conference*. pp. 155–171.

SAE, S. of A.E., 2007. *Instrumentation for Impact Test-Part 1-Electronic Instrumentation*, Warrendale, PA.

Schafman, M.A. et al., 2016. Age and sex alone are insufficient to predict human rib structural response to dynamic A-P loading. *Journal of Biomechanics*, 49(14), pp.3516–3522. Available at: http://dx.doi.org/10.1016/j.jbiomech.2016.09.030.

Yoganandan, N. et al., 1995. Thoracic Deformation and Velocity Analysis in Frontal Impact. *Journal of Biomechanical Engineering*, 117(1), pp.48–52.

Yoganandan, N., Arun, M.W.J. & Pintar, F. a., 2014. Normalizing and Scaling of Data to Derive Human Response Corridors from Impact Tests. *Journal of Biomechanics*, 47(8), pp.1749–1756. Available at: http://dx.doi.org/10.1016/j.jbiomech.2014.03.010.